IJIRCCE

e-ISSN: 2320-9801 | p-ISSN: 2320-9798

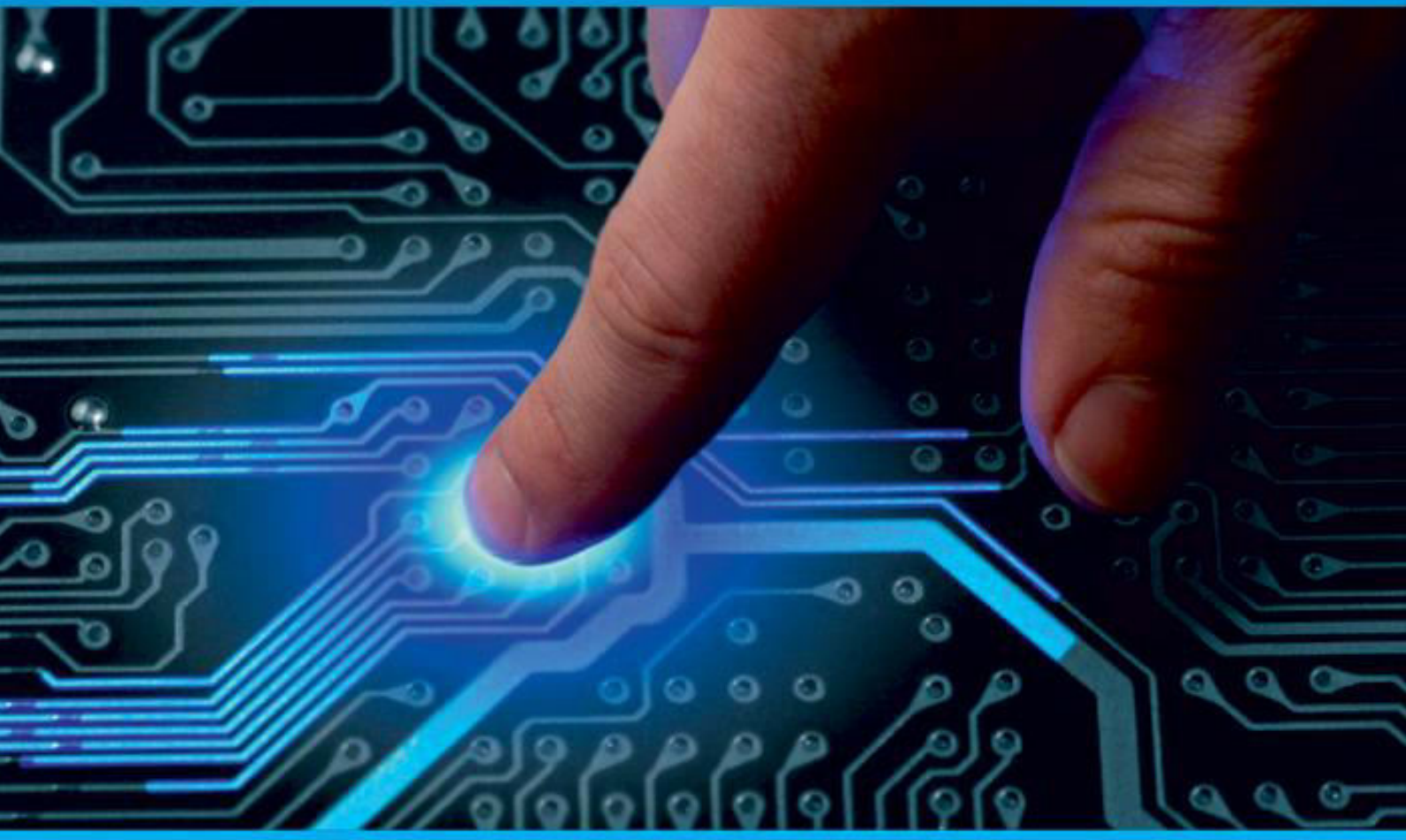

INTERNATIONAL JOURNAL OF INNOVATIVE RESEARCH

IN COMPUTER & COMMUNICATION ENGINEERING

Volume 10, Issue 9, September 2022

INTERNATIONAL STANDARD SERIAL NUMBER INDIA

Impact Factor: 8.165

International Journal of Innovative Research in Computer and Communication Engineering

| e-ISSN: 2320-9801, p-ISSN: 2320-9798| www.ijircce.com | |Impact Factor: 8.165

|| Volume 10, Issue 9, September 2022 ||

| DOI: 10.15680/IJIRCCE.2022.1009031 |

An Efficient Deep Neural Network Framework for Detecting and Removing Specular Highlights from Hyperspectral Images

[1]Abdussalam Mohamed Ali Altaher, [2]Aimn Azoumi Mohammed, [3]Massoud Ali Abdalhadi

Department of Information Technology, Higher Institute of Science and Technology, Wadi Al-Ajal, Libya

ABSTRACT: When any type of illumination from the illuminating source falls on an object with a smooth surface, the light rays tend to scatter and form a reflection called an imagehighlight. These highlights in the images will reduce the quality of the image and the details. This removal of highlights from the image is very much required in the medical field, with the intent to improve the quality of cardiac and endoscopic images. Highlights in these images will make the particulars unclear and proper therapy cannot be given. This paper deals with the removal of highlights from hyperspectral images.Several methods are so far implemented for the removal of highlights.But these methods lack efficiency, and accuracy and cannot process a large number of datasets. Aiming at these difficulties in the previous methods, there is a requirement for a method that can overcome such difficulties. Therefore, optimized deep learning is introduced in this paper in which the reflectance in the hyperspectral images is detected by the artificial intelligence-based Convolutional Neural Network (CNN) method, which provides superior improvement. Ant Colony Optimization based Convolutional Neural Network (ACO-CNN)mechanism's novel constraintsare implemented in this paper. For the removal of highlights from the hyperspectral image, this model has been established and bestowed cooperatively with a dataset that contains many images. The outcome exhibit that the developed framework outperforms the contemporary methods by providing higher accuracyin the removal of specular highlights from hyperspectral images.

KEYWORDS: Specular Highlight Removal, Deep Learning, Ant Colony Optimization, Convolutional Neural Network

I. INTRODUCTION

Highlights are most commonly found in any objects with polished surfaces and less texture. Due to their very glossy surface, the highlights are formed. Image acquisition is affected by the formation of these reflectance highlights on the surface of the objects. These reflectance highlights will affect the quality of the image. So there is an emerging need to remove those highlights from the images by introducing several techniques. Image highlight removal is necessary for so many fields including cardiac images, endoscopic images, different perspectives of facial images, real-time vision-based systems, etc. The pretentious areas are determined by edge detection[1]. The quality of fresh fruits is also checked by this method in such a way that the labor cost is reduced [2]. For carrying out this highlight removal process, datasets are collected and a suitable type of algorithm like the body reflection essence neuter model is adapted[3]. Highlight removal methods can be based on a single image and multiple images. Surface normal and lighting directions can be obtained from the extracted reflectance highlight. Since this reflectance from the object due to an illuminating source is unavoidable, it can lead to the deduction of many particulars in the image which results in poor medical results, computer vision, etc. To overcome such difficulties, highlight removal is mandatory to attain the maximum quality of the images.

The dynamic searching and classification found the areas with indistinguishable structure features to reflectance areas. Eventhough the accuracy is high, this method failed to explain the feature extraction [4].Although the fact that the vision-based systems can control high-quality videos, it shows poor computational complexity [5].Highlight removal techniques can be classified based on the number of images used. The removal of highlights using a single

| e-ISSN: 2320-9801, p-ISSN: 2320-9798| www.ijircce.com | |Impact Factor: 8.165

|| Volume 10, Issue 9, September 2022 ||

| DOI: 10.15680/IJIRCCE.2022.1009031 |

image is much more difficult than the multiple images because there is a requirement for color segmentation in a single image [6].There are numerous numbers of works are being carried out in the past to remove the highlights in the images using Support Vector Machine (SVM) and other techniques that use machine learning. But these techniques can only process limited numbers of datasets and in most cases, the accuracy is imperfect [7].So, there is a need for a technique thatcan process a large number of datasets. This study investigates the removal of highlights from the image using a deep learning technique.

CNN is a mechanism that is derived from the visual perspective of living creatures which makes the classification process simple [8]. A deep learning technique called Convolutional Neural Network (CNN) is introduced to process a large number of datasets. CNN is also efficient computationally.It carries out parameter sharing, particular convolution, and pooling operations. CNN models may now be used on any device and are accepted by everyone as a result.CNN has numerous applications like finding the homogeneity of the material, pattern recognition, image processing, etc.[9].

The detection of highlights in hyperspectral images has been implemented using an Ant Colony method. An optimization session using ant colony behavior is known as an ant colony optimization [10].An artificial ant that employs straightforward computations of an agent to find a more effective solution to the problem is used in an ant colony optimization technique. The maximum and minimum concentrations of pheromones on each trail are controlled by an ant colony algorithm. As a result, when a limited number of ants travel, pheromone departure is lower on shorter routes than it is on longer ones [11]. The shortest paths are used to collect the most pheromone. This implies that as more pheromone attracts more ants, all the ants will finally discover the shortest route. The given problem is intended to be transformed into the problem of locating the optimal path for the complex problem in this algorithm. Each ant discovers a solution in the initial stage of duplication.

The key contribution of the developed framework is summarized as:

- Initially, a large number of hyperspectral images with highlights are collected and processed in the system
- Furthermore, the restored hyperspectral images contain additional noise, which is filtered using a hybrid filter called the Weinmed filter.
- The adopted segmentation process in this paper is ant colony optimization.
- Feature extraction is carried out byGLCM.
- The ACO-CNN detects the highlighted region from the hyperspectral image.
- The achievement of the implied method is approved and associated with existing approaches to show its effectiveness.

The remainder of this essay is organized as follows: The pertinent works are presented in Section 2 along with a thorough analysis of them. Section 3 contains information about the problem statement. The proposed ACO-CNN architectures are explored in detail in Section 4. In Chapter 5, experiment findings are presented, and reviewed, and a thorough assessment of the suggested strategy in comparison to current best practices is made. Section 6 is where the document is completed.

II. RELATED WORKS

Yefei Gao et al. [4] employed highlight removal by dynamic searching and classification. The separation and restoration of a specific region from a single image are accomplished in this paper. Here the separation is carried out by introducing a learning classification algorithm called SVM which separates the highlight pixels by considering it as a binary problem. The restoration is done by multi-scale dynamic image expansion and fusion method thereby the highlights in the image are removed. The implemented highlight method comprises pixel-wise feature construction, structure-wise attributes construction, and multi-scale dynamic searching. The areas with indistinguishable structure features to reflectance areas are determined by this method. The study reveals that the

| e-ISSN: 2320-9801, p-ISSN: 2320-9798| www.ijircce.com | |Impact Factor: 8.165

|| Volume 10, Issue 9, September 2022 ||

| DOI: 10.15680/IJIRCCE.2022.1009031 |

separation accuracy is higher than recurrently used techniques. However, feature extraction is left incomplete in this paper.

Samar et al. [1] implemented highlight removal in cardiac images using an automatic and robust single camera. The pretentious area is found by hybrid color characteristics and wavelet-based edge projection. These regions are then retrieved by dynamic search-based techniques. This detection method does not depend on the properties of the target or attributes of the source that illuminates it. The computational time of this method is low which makes the correction process very efficient. However, this study didn't explain the accuracy rate.

Vitor et al. proposed highlight removal for pipelines [3]. This paper depends on the body reflection essence-neuter which is carried out in real-time. Global image statistics and point-wise intensity transformations are used in this method. The body reflection essence-neuter model is used for determining the color, deteriorating the inherent image, and in computer graphics. This model differentiates the diffuse and specular reflections. The suggested approach produces the desired outcomes with little computational expense, enabling it to be used in systems with little processing capacity. Although the paper does not explain the saliency, sparse modeling, and highlight removal in videos.

Tong et al. [7] implemented an optimization method for the highlight removal of different perspectives of facial images. The lightweight optimization method is used for removing highlights in facial images. The Lambertian consistency asserts that the scattered element does not change in the observing angle, while there is a change in behavior in the specular component. In this technique, the illumination chromaticity is estimated for highlight removal by introducing orthogonal subspace projection. Laboratory captured datasets with ground truth and FaceScape datasets are collected and are employed in this method. Non-negative constraints and orthogonal subspace projection are used to execute the pixel-wise optimization. This method exhibits improved accuracy than the other methods. Nevertheless, there is a requirement for sufficient datasets for better results.

Dat et al. [5] employed real-time vision-based systems for single-image haze removal. In this paper, real-time processing is made easier by the introduction of hardware that correlates with the single image haze removal algorithm. This haze removal algorithm can be classified into single and multiple image algorithms. The single image algorithm includes image restoration and image enhancement. Koschmieder model is executed in this paper and the use of low visibility images for haze removal is deduced. To bring the deduction into effect, the details are improved and gamma correction is done. This method can control high-quality videos. Even though this method is effective, the computational complexity is very poor.

Jinglei et al. [2] proposed an algorithm for checking the uniformity, firmness, and, maturity of fresh fruits. A reflectance removal algorithm based on multi-band polarization imaging is implemented in this paper. This method involves capturing an image and reflectance removal. The shadowy and dispersion information of the target is obtained by image acquisition to achieve a multi-spectral dispersion imager with a different arrangement. Then the specular highlights are removed accurately to introduce the reflectance removal method based on multi-spectral. This method shows improved results in the visual outcome and image resolution when compared with other algorithms. Better accuracy and complexity can be achieved in this method. However, the effectiveness of this method is left undiscussed.

High-quality highlight removal was proposed by Jinli et al. [12]. The clarity in saturation and respective bicolored model is used to remove the highlights from the image in a fast and effective way. In this paper, a normal bicolored model is obtained for the pixels with the same dispersed color. An equation of projection coefficients in a unit circle for two subspaces that are, respectively, orthogonal to and parallel to the illumination. Specular-free former illumination orthogonal subspace enables durable clustering with a defined parameter to dynamically decide the cluster number. A characteristic known as PDDR aids in mapping each specularly influenced pixel to its diffuse element in the second illumination parallel subspace.As a result, the suggested method can quickly remove highlights from high-resolution photos while requiring a few complicated calculations. Experiments demonstrate

| e-ISSN: 2320-9801, p-ISSN: 2320-9798| www.ijircce.com | |Impact Factor: 8.165

|| Volume 10, Issue 9, September 2022 ||

| DOI: 10.15680/IJIRCCE.2022.1009031 |

that this approach is of better results in a variety of difficult scenarios. Despite that, the calculation involved in this method is difficult and consumes time.

Pixel clustering is the technique used in this paper for the removal of specular highlights which was proposed by Antonia et al. [13]. In this paper, specular highlights can be instantly removed from one image using a high-quality pixel clustering technique. While offering the most accurate results for three of the four images available in the present dataset for specular highlight reduction, the proposed approach can process data two times faster than the state-of-the-art.It was accomplished by combining a simple but efficient pixel clustering algorithm with an improved method to distinguish diffuse from specular pixels. Furthermore, even for 2160p image resolutions, it can deliver real-time performance for the removal of specular highlights by GPU-based technology. However, accuracy is not discussed in this paper.

Correcting hyperspectral and color images while identifying the distortion model is discussed in this paper by Arten et al. [14]. As an existing understanding for identification, image patches with consistent qualities over affected and distortion-free images or image sections are used. Finding a matched distortion-free element for each warped spectrum shape element is the key challenge during previous knowledge representation. The search for a matching spectrum shape element is theoretically supported by the presentation of a requirement. This essential condition served as an optimization constraint while we used RANSAC to solve the detection problem.The technique is effective for both hyperspectral and color images. However, pixel and sensor noise sampling was not taken into account.

Wenyao et al. [15]proposed an optimization technique for the removal of highlights. The texture of the highlights varies in natural lights.A dichromatic reflection model-based optimization method for specular highlight removal is proposed in this paper. In addition to modified illumination chromaticity, the proposed method also includes two novel steps: the first correct color and saturation on highlighted regions to estimate diffuse chromaticity and the second uses convex optimization with double regularization to estimate diffuse and specular reflection coefficients. It has been demonstrated that the calculated diffuse chromaticity is close to the actual diffuse chromaticity, and the suggested optimization process will always yield the best diffuse coefficients. The suggested method may successfully eliminate specular highlights from both natural and endoscopic images while preserving the detail, according to experimental findings. Although the accuracy of this method is low.

III. PROBLEM STATEMENT

The former studies concentrated on binary classification problems which can be resolved bythe Support Vector Machine (SVM) algorithm in machine learningfor recognizing and surveying the highlights in the image. Nevertheless, this binary classification problem with SVM cannot process plenty of datasets because the needed preparation time is higher and has low accuracy. The SVM cannot accomplish its function properly when the noise in the datasets is higher and the computational complexity of the SVM algorithm is also poor. So, it may affect the quality of the image which results in unfocused endoscopic and cardiac images and may source health warnings to patients.So, to achieve better results, the method which can process a large number of datasets with good accuracy and efficiency is vital. Deep learning has the ability to perform the indefinite data well, it is cost-effective and can process a large number of resources. Thus, the image highlights are removed by implementing advanced deep learning methods. Here, the Ant Colony Optimization-based Convolutional Neural Network (CNN) is employed.

IV. PROPOSED ACO-BASED CNN

The proposed method is outlined in figure 1. Ant Colony Optimization based Convolutional Neural Network is employed in this study. Several datasets are fed into the system for the training and testing process. Then the images with highlights are subjected to preprocessing in which the median filter is applied to take off the undesirable noises from the images. Correspondingly, the accepted ACO-CNN technique is used to classify the image highlight and its categories. Furthermore, an advanced Ant Colony Optimization-based Convolutional Neural

| e-ISSN: 2320-9801, p-ISSN: 2320-9798| www.ijircce.com | |Impact Factor: 8.165

|| Volume 10, Issue 9, September 2022 ||

| DOI: 10.15680/IJIRCCE.2022.1009031 |

Network is employed to obtain a superior precision value. Hence the adopted technique contemplates and categorizes the highlights in the image.

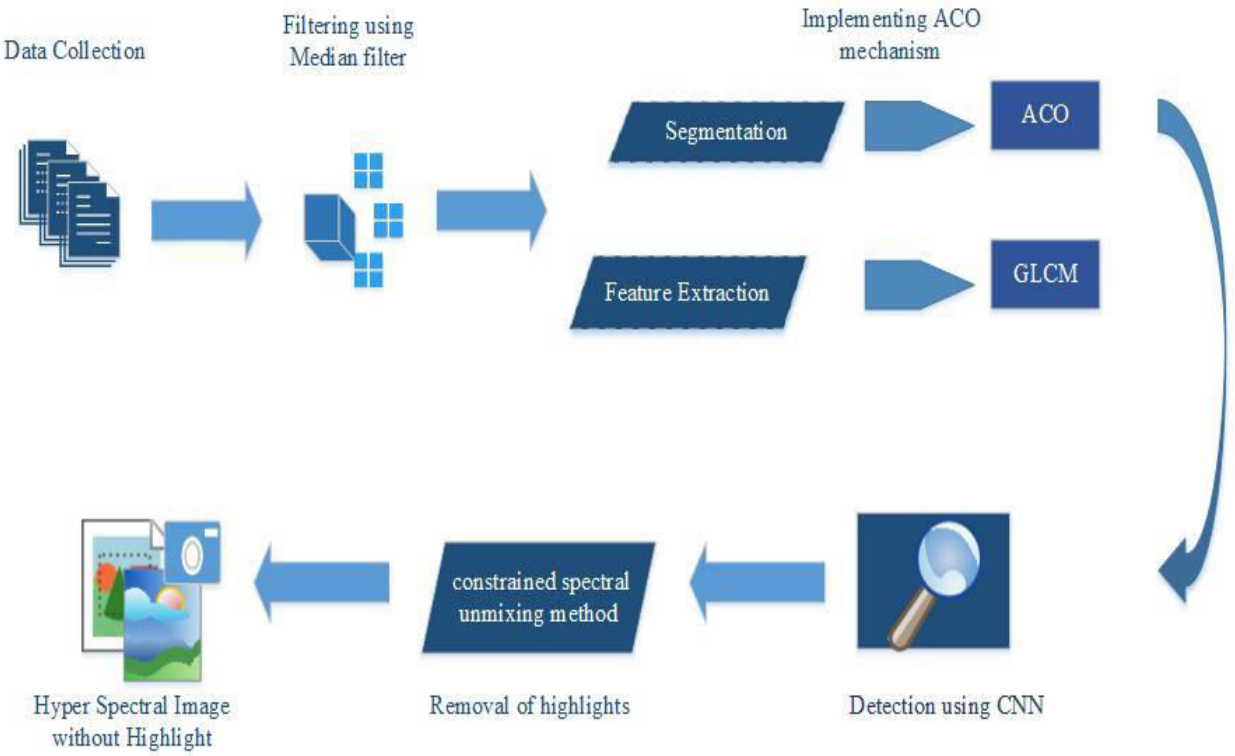

Figure 1: **Proposed ACO-CNN method**

4.1 Data Collection

Nearly 10,000 datasets including cardiac and endoscopic images with highlights are been collected and used in this experimentation. From these 50% of images are used as training data and 50% of images are used as testing data. That is to say that 5000 hyperspectral images with highlights are taken as training data and 5000 hyperspectral images with highlights are taken as testing data.

4.2 Preprocessing

Preprocessing is carried out to receive an image with appreciable pictorial clarity. The most common noise faced by the images is salt and pepper noise which makes the highlight removal process difficult [16]. To exactly recognize there flectance regions, an identification process that is based on global and local analysis is put forward. A local analysis compares the image's intensity and saturation to a global analysis, which examines the image's color properties. Any arrival of unintended signs and imbalance in luminosity and tint of the image is called noise. As the grains will affect the quality of the image, it is necessary to get rid of the noises. Accordingly, to reduce the noise in the images, a hybrid filter with a combination of wiener and median called the Wienmed filter is used in this research. The median filter is very effective in sorting out spiky noises while preserving the sharp edge characteristics of the image and it will also restore the gray level of each pixel. On the other hand, the wiener filter is the linear filter for blurring the noise in the image. So, combining the median and wiener filter is found to be very much effective and it is employed in this paper. To attain an improved quality of image, the altered pixels from the surroundings have to be removed [17]. Hence the obtained noiseless images are utilized in the ACO-CNN model for the removal of highlights from the image.

| e-ISSN: 2320-9801, p-ISSN: 2320-9798| www.ijircce.com | |Impact Factor: 8.165

|| Volume 10, Issue 9, September 2022 ||

| DOI: 10.15680/IJIRCCE.2022.1009031 |

The equation for the wiener filter is,

$$w(p, q) = \sigma^2[n - a(p, q)] \quad (1)$$

Here σ^2 is the variance of Gaussian noise, p and q are pixel dimensions of each image, n is the noise features.

The equation for the median filter is,

$$\hat{g}(a,b) = median_{(x,y)\in T_{ab}}\{f(x,y)\} \quad (2)$$

Here $f(x,y)$ remaining pixel after removal.

The combined equation proposed for the Wienmed filter is,

$$\hat{g}(a,b) = median_{(x,y)\in T_{ab}}\{w(p,q)\} \quad (3)$$

Here p and q are the pixel dimensions of each image. Each image is denoted by a.

4.3 Segmentation using ACO

The segmentation process is mostly done for segmenting the reflectance regions from the hyperspectral images. The success of the image segmentation process will determine the capability of superior level removal of highlights from the hyperspectral image. Initially, the hyperspectral image has to be classified as a region under normal light and the highlighted region [18]. The pixels in the hyperspectral images are broken down into an undeviating combination of pure spectra [19]. Highlights from the hyperspectral image are segmented with an advanced CNN-based Ant Colony Optimization algorithm applied in this proposed method.The spectral bands in the hyperspectral images are utilized in the process of segmentation to understand their characteristics [20]. The hyperspectral image is split into pixel sets or several divisions and labels are given to each pixel in the image segmentation process. Certain attributes were assigned by several pixels that have labels relatively.

Ant Colony optimization algorithm

Nowadays, the approach of Ant Colony Optimization is applied for approximative optimization. The Ant Colony Optimization is driven by the ant's searching activity. The primary method of communication used by ants allows them to locate the fastest route to their food source. The Ant Colony Optimization technique (ACO) uses this ant's unique trait. Here ACO is used to detect the highlights from the hyperspectral image. The pheromone rate is one of the crucial characteristics in the database that needs to be changed first. All of the relevant material used to investigate the feature is contained in a matrix (h) with a dimension of G*G, where G is the number of unique feature vectors in its rows and columns. The primary calculation, such as the experimental function F, is calculated after modifying the ant colony optimization settings. Identify the best-constrained subset and resources for the upcoming repetition.

The initialization of its factors is the first and most crucial step in putting the Ant Colony Optimization algorithm into practice. There are lots of candidate ants in it. Strong toughness and an isolated calculative process are also features of the ACO algorithm. ACO is easily interchangeable with other techniques and performs admirably when it comes to solving challenging optimization issues. The updated pheromone is used by ACO, and ants move in the search area following mathematical formulas. Local and global searches are the foundation of ACO.

Transition probability of region (m)

The formula for calculating a region's transition probability is utilized to determine where the specular highlight is located.

$$Q_a(s) = \frac{s_a(s)}{\sum_{i=1}^{d} s_i(s)} \quad (4)$$

Here $s_a(s)$ represents the total pheromone at region *a* and *d* is the number of global ants.

The Equation for pheromone update

An ant releases a substance called a pheromone that modifies the behavior of other ants.The equation for the pheromone update used by ants to communicate is,

$$p_j(p+1) = (1-s)p_j(p) \quad (5)$$

Here 's' denotes pheromone evaporation rate.

| e-ISSN: 2320-9801, p-ISSN: 2320-9798| www.ijircce.com | |Impact Factor: 8.165

|| Volume 10, Issue 9, September 2022 ||

| DOI: 10.15680/IJIRCCE.2022.1009031 |

Edge traversed equation

All the ants update the local pheromone after each construction stage. Each ant only uses it on the most recent edge they crossed.

$$\tau_{ij} = (1 - \Psi) . \tau_{ij} + \Psi . \tau_0 \quad (6)$$

4.4 Feature extraction

The selection of certain attributes from the given set of characteristics is the major problem in image processing technology. Identification of design, contents, and image are the disciplines of image processing in which feature extraction is applied. Attributes of the hyperspectral image may includeform, change of color, dissimilarity, group protrusion, the connection among the space, etc. [11]. Feature extraction in image processing aims to lessen the computational complication by eliminating ineffective and superfluous attributes.The attributes of the images are determined in the feature extraction process which includes microanalysis and macro analysis [18]. In feature extraction, the source data is converted into digital features without making any changes in the eccentric datasets and it is categorized based on its pixel.

Gray Level Co-occurrence Matrix (GLCM) is applied in feature extraction. By calculating how frequently a pair of pixels with specific values and spatial relationships appear in an image, the GLCM factor represents the texture of an image.For removing the statistical texture feature, correlation, energy, homogeneity, contrast, entropy, etc. are evaluated as second-order image characteristics.

Energy

Energy is defined as the sum of squares with grayscale values that are often higher and have erratic concentration values in images. The energy of input data is calculated in Eqn. (7)

$$E = \sum_{p}\sum_{q}\{M(p,q)\}^2 \quad (7)$$

Where the images are denoted as M, and the image's squares with grey levels are labeled as (p, q).

Contrast

Features are used to measure the local contrast of an image, and it is predicted to be low while in the even concentration value. The original image's total grayscale content is then projected, according to Eqn. (8), followed by the contrast.

$$C = \sum_{y=0}^{I_q} y^2 \left\{ \sum_{p=1}^{I_q}\sum_{q=1}^{I_q} M(p,q) \right\} \quad (8)$$

I stand for the grayscale of the images, M for the images, and (p, q) for the square of an image's grayscale.

Correlation

By making use of the correlation characteristics shown in Eqn. (9), it is possible to take into account the numerical relationships between the variables as well as the linear dependence of grey levels on the pixels.

$$C_o = \frac{\sum_{p}\sum_{q}(p,q)M(p,q) - \mu_u\mu_v}{\sigma_u\sigma_v} \quad (9)$$

In the images, the values of mean, as well as standard deviation, are μ_u, μ_v, σ_u, *and* σ_v are characterized as row and column.

Entropy

Entropy, which is indicated in Eqn. (10), stands out as the expected high value of the randomization of the allocation of grey levels.

$$En = -\sum_{p}\sum_{q} M(p,q)\log\left(M(p,q)\right) \quad (10)$$

4.4.1 Detection using CNN

The highlights in the hyperspectral images are recognized using the Convolution Neural Network (CNN) classifiers. Its multi-layered design effectively analyses graphical images and eliminates the necessary features. Image input, convolutional layer, Max pooling layer, fully connected layer, and output are the four layers that make up the CNN classifier. The dataset's range of hyperspectral image pixel intensities before convolution neural

| e-ISSN: 2320-9801, p-ISSN: 2320-9798| www.ijircce.com | |Impact Factor: 8.165

|| Volume 10, Issue 9, September 2022 ||

| DOI: 10.15680/IJIRCCE.2022.1009031 |

network training. CNN is the model that runs the fastest throughout training. The size of the images which are given as input should be uniform. Formula or the normalization of each image in the training set is given in Eqn. (11)

$$p(u,v) = \frac{O(u,v)-\mu}{\sigma} \quad (11)$$

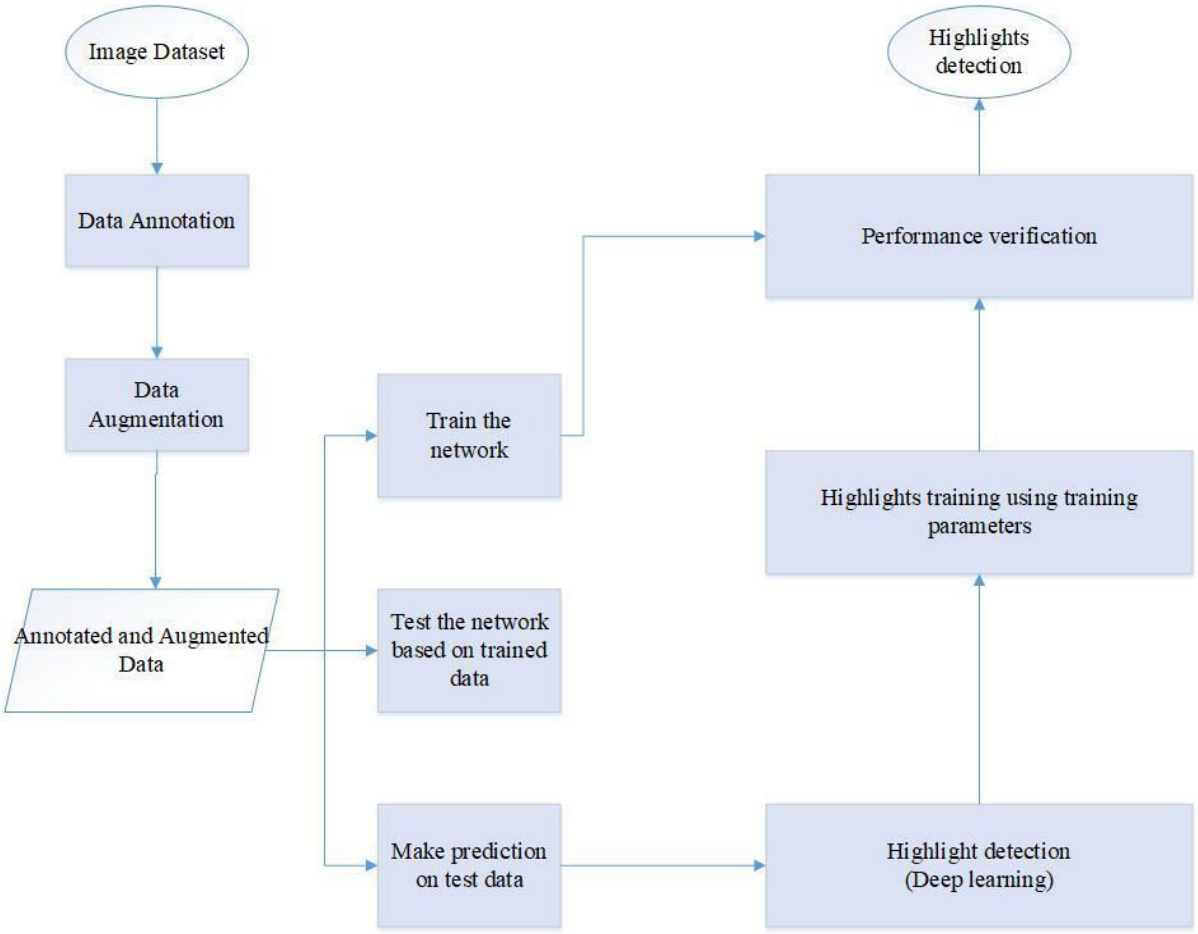

Figure 2: **Working of CNN**

Figure.2 explains the working of a Convolutional Neural Network where several datasets are given as input images. Then the annotated and augmented data is trained and testing is done based on the training. After prediction, the highlights are detected.

a) Convolutional layer

The convolution layer gathers a few images as input and uses each layer to analyze the complexity of each of them. It is directly related to the characteristics we are looking for in the provided images.

$$f_i^n = x(\sum_{j \in N_i} f_j^{n-1} * p_{ji}^n + x_i^n) \quad (12)$$

N_i –it represents an input selection. An additive bias v has been given as an output. The kernel applied to map i, if the total of the maps j and k over map i.

| e-ISSN: 2320-9801, p-ISSN: 2320-9798| www.ijircce.com | |Impact Factor: 8.165

|| Volume 10, Issue 9, September 2022 ||

| DOI: 10.15680/IJIRCCE.2022.1009031 |

b) Max pooling layer

The fitting and neuron size utilized in the downsampling layer are reduced by this layer. The Pooling layer cuts down on the number of parameters, computation rate, size of the feature map, training time, and overfitting. 50% of test data and 100% of the training dataset are the criteria for overfitting.

$$x_{nuv} = nux_{(s,t)\in} f_{nst} \quad (13)$$

Map,f_{nst} is the element at (*s, t*) within the pooling region p_{uv} which represents a local neighborhood around the place (*u, v).*

c) Fully connected layer

A fully Connected Layer has been utilized in the context of image categorization. All of the Convolution layers are put before the FC layers. The mapping of the illustration between the input and output is facilitated by the FC layer. The final levels of the network are fully connected layers. The fully connected layer receives its input from the max pooling layer's output.

d) Softmax layer

The scores are transformed into a normalized probability distribution using the Softmax layer. Any type of highlights in the hyperspectral image is detected in this layer. It can be expressed in the following Eqn, (14),

$$\sigma(\vec{X})_m = \frac{e^{x_m}}{\sum_{i=1}^{m} e^{x_i}} \quad (14)$$

4.5 Removal of highlights

After detecting the highlights from the image, a method that depends on constrained spectral unmixing is used to remove the highlights. To eliminate highlights from a single spectral image, we describe a limited spectral unmixing technique [22]. The constraints for the constrained spectral unmixing approach have been set up so that all diffuse and highlight reflection fractions add up to 1 and are positive. As a result, the diffuse image's spectra are always positive. The pure highlight spectrum has been taken from the light source's spectral power distribution (SPD). Out of the collection of diffuse spectra, the measured spectrum's pure diffuse spectrum was selected. An automated target generation algorithm has extracted the collection of diffuse spectra from the image's diffuse region. The highlight and diffuse portions of the image have been identified using constrained energy reduction in a limited impulse response linear filter.

a) Orthogonal subspace projection

A Matched Filter is then used to match the desired target from the data using Orthogonal Subspace Projection (OSP), which first builds an orthogonal subspace projector to exclude the response of non-targets. When target signatures are distinct, OSP is effective and efficient. Here three-dimensional objects can be represented in two dimensions.The orthographic projection is not equal-area or conformal. In general, distortions exist in areas, lengths, orientations, and angles. Only the map's center is distortion-free. Radially outward from the origin, distortion values significantly rise.

The OSP is a widely used hyperspectral imaging method that has a wide range of applications[23].Popular anomaly detectors like the orthogonal subspace projection (OSP) detector build backdrop subspace using local endmembers and eigenvectors around the PUT. However, this subspace only utilizes the spectral data and ignores the way that the background noise is spatially correlated, making the anomaly detection result susceptible to the estimated subspace's accuracy. The three associated orthogonal subspaces are determined. Following that, the local cube's three directions are projected for each of the vectors.

b) Probabilistic PCA

Data analysis using a lower dimensional latent space is done using the dimensionality reduction approach known as probabilistic principal components analysis (PCA).A chapter on principal component analysis (PCA), a well-known method for dimensionality reduction, may be found in many multivariate analysis texts. Image processing is one of the applications of PCA. A standardized linear projection is the most popular way to derive PCA.

| e-ISSN: 2320-9801, p-ISSN: 2320-9798| www.ijircce.com | |Impact Factor: 8.165

|| Volume 10, Issue 9, September 2022 ||

| DOI: 10.15680/IJIRCCE.2022.1009031 |

A tried-and-true method of dimensionality reduction is PCA[24]. It was suggested to use PPCA, PCA, and the K-nearest algorithm to remove highlights from one spectral image.The data for the body cluster and the highlighted cluster were clustered using PPCA. The K nearest-neighbor algorithm used in the method in causes highlight elimination in the spectral image by swapping out highlight pixels with body reflection pixels.

c) Spectral unmixing

Decomposing a mixed pixel's spectral signature into a group of endmembers and their respective abundances is the process of spectral unmixing. Endmembers are the pure components in the image that make up their spectra, and amplitudes at each pixel show how much of each endmember is present there. The spectral unmixing problem is addressed using solely the spectrum features of the image since many spectral unmixing approaches assume a pixel as irrespective of its neighbors[25].

A technique for subpixel analysis is spectral unmixing. A widely used method for mixed pixel categorization in spectral imaging is linear restricted spectral unmixing. The spectrum is the linear combination of the pure target fingerprints in linear spectral unmixing. The approach estimates the target material fractions for each pixel spectrum. The target signatures used in highlight removal from spectral images are the signatures of the highlight component and the diffuse component.The proposed highlight removal technique for spectrum imaging appears promising.

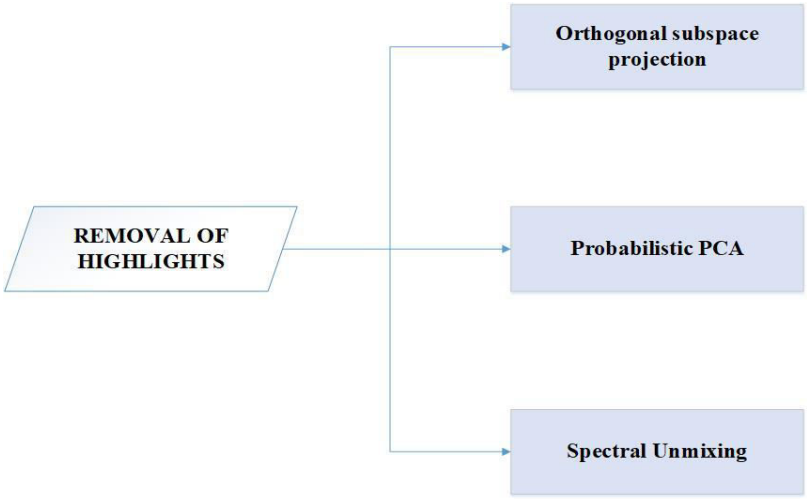

Figure 3: **Removal of highlights**

Figure.3 shows the steps in the removal of highlights. Orthogonal subspace projection, probabilistic PCA, and spectral unmixing are the steps in the removal of highlights from hyperspectral images after the detection process.

Algorithm: ACO-CNN mechanism

Input: *Hyperspectral images with highlight*
Output: *Detection of highlights from Hyperspectral images*
Load input image data
$I = \{I_1, I_2, I_3 \dots\}$ *// data acquisition*
Pre-processing of images *//wienmed filter*
$\hat{g}(a,b) = median_{(x,y)\in T_{ab}}\{w(p,q)\}$
Segmentation of images *// Ant Colony Optimization*

| e-ISSN: 2320-9801, p-ISSN: 2320-9798| www.ijircce.com | |Impact Factor: 8.165

|| Volume 10, Issue 9, September 2022 ||

| DOI: 10.15680/IJIRCCE.2022.1009031 |

```
        Initialize the starting pointof the highlighted portion
        if (ant reaches the next position)
                Gather the subset
                Identify the highlights in the hyperspectral image using Eqn. (4)
        Else
                Find out the next component using Eqn. (5)      //update pheromone
                Repeat until a stopping criterion is met
        end if
Return
Feature extraction                                              //GLCM
Detection of highlights in Hyperspectral images                 //CNN Classifier
Removal of highlights in Hyperspectral images                   //Constrained spectral unmixing
```

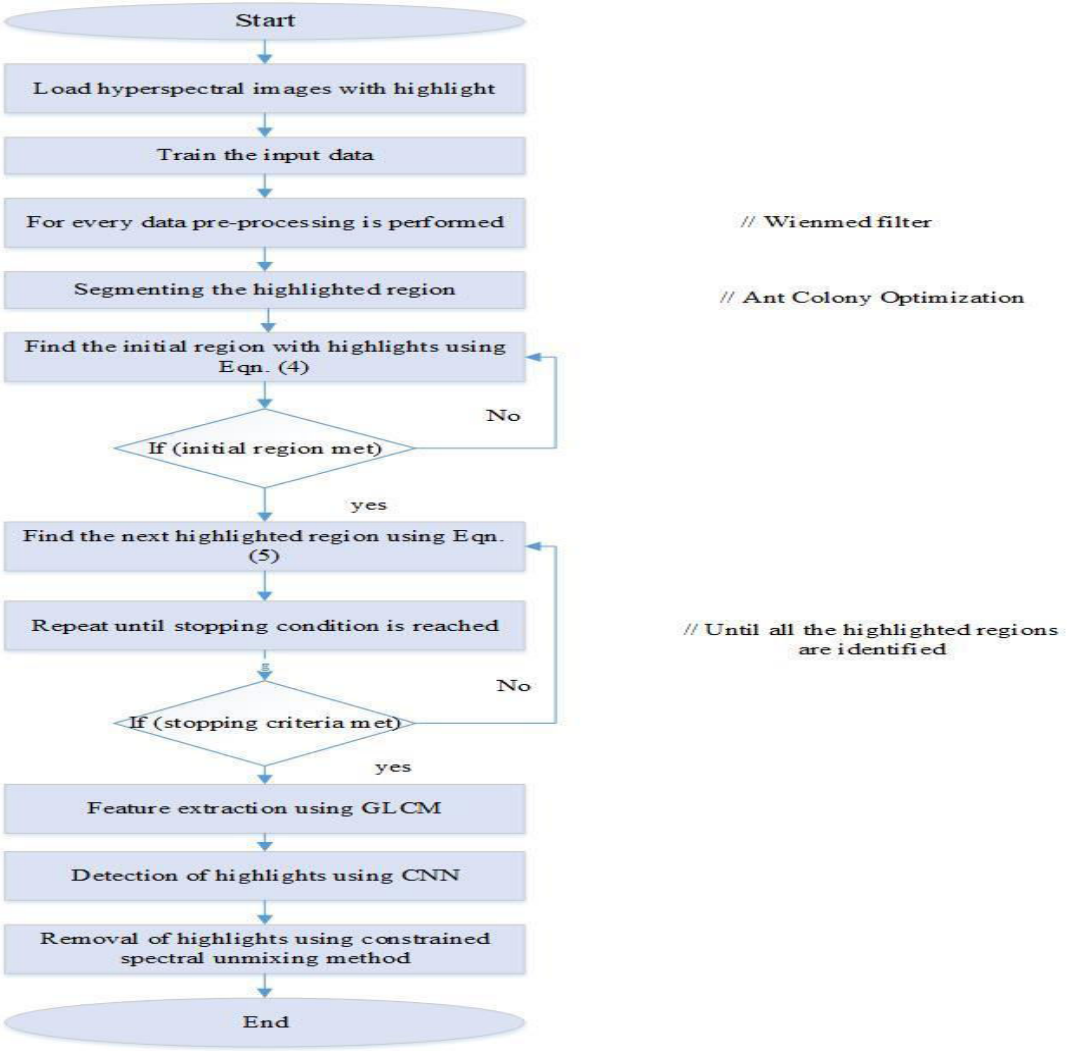

Figure 4:**Flow diagram of ACO-CNN model**

| e-ISSN: 2320-9801, p-ISSN: 2320-9798| www.ijircce.com | |Impact Factor: 8.165

|| Volume 10, Issue 9, September 2022 ||

| DOI: 10.15680/IJIRCCE.2022.1009031 |

The complete flowchartfor detection of highlights from the hyperspectralimage is shown in figure.4. The flowchart starts with the loading of hyperspectral images with highlights. Then the images that are given as input were trained. Weinmedd filter is introduced in pre-processing stage to remove any type of unwanted noise from the image. These images without noise are used in the segmentation process. The proposed ABO-CNN is utilized in the process of segmentation. Eqn. (4) is used to find the initial region with highlights. Eqn. (5) is used to find the next highlighted region, if the initial highlighted region is found. If the initial highlighted region is not found go back to Eqn. (4) until the initial highlight is found. After detecting the next highlighted region, repeat eqn. (5) until the stopping criteria are met. Then feature extraction is carried out if the stopping criteria are met. GLCM is applied in the feature extraction process to find the correlation, contrast, entropy, and energy of the images. Then the CNN is used to detect the highlights from the hyperspectral images.

V. RESULT AND DISCUSSION

By using the datasets of hyperspectral images,the planned method has been investigated. The Ant Colony Optimization–based CNN is implemented to detect the highlights from the hyperspectral images. The exposition of the intended model is assessed through operating parameters such as Accuracy, Precision, Recall, and F-measure.

5.1 Accuracy

Accuracy is the degree of proximity between a calculation and its true value. It is the ratio of correctly calculated data to the total number of measurements. Accuracy is expressed in Eqn. (15),

$$Accuracy = \frac{T_{Pos} + T_{Neg}}{T_{Pos} + T_{Neg} + F_{Pos} + F_{Neg}} \tag{15}$$

5.2 Precision

Precision is the degree of proximity between two or more calculations and it also refers to the quality of being exact. Precision depends on the accuracy and shows how repeatable a measurement is. Precision can be computed from Eqn. (16),

$$P = \frac{T_{Pos}}{T_{Pos} + F_{Pos}} \tag{16}$$

5.3 Recall

Recall refers to the percentage of total appropriate results correctly grouped by the algorithm. It is defined as the ratio of right positive to the true positive and false negative values. It is uttered in Eqn. (17),

$$R = \frac{T_{Pos}}{T_{Pos} + F_{Neg}} \tag{17}$$

5.4 F1-Score

The F1-score calculation is the combination of precision and recall. The values of precision and recall play a vital role in calculating the F1score. It is represented in Eqn. (18),

$$F1-score = \frac{2 \times precision \times recall}{precision + recall} \tag{18}$$

Table1:**Performance evaluation based on ABO-CNN**

	CNN	ACO-CNN
Training accuracy	99.4	99.8
Testing accuracy	97.6	98.9

| e-ISSN: 2320-9801, p-ISSN: 2320-9798| www.ijircce.com | |Impact Factor: 8.165

|| Volume 10, Issue 9, September 2022 ||

| DOI: 10.15680/IJIRCCE.2022.1009031 |

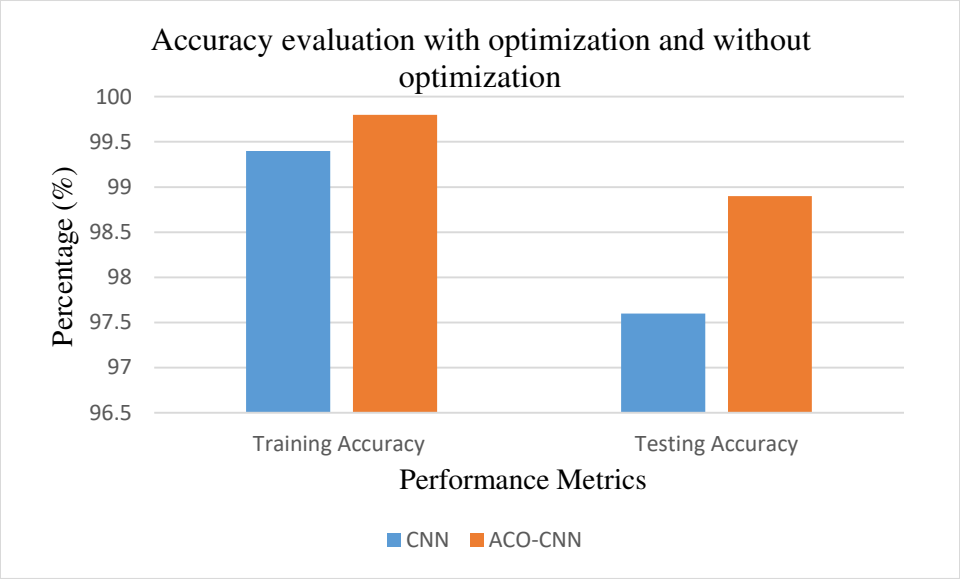

Figure 5:**Accuracy evaluation with optimization and without optimization**

Table 1 shows that for the testing and training process the accuracy of the Convolutional Neural Network is 99.4% and 97.6%. While using Ant Colony Optimization, the accuracy of the testing and training process increases to 99.8% and 98.9% correspondingly.

Table2:**Comparison of accuracy in the performance matrix**

Method	**Accuracy (%)**
Dynamic searching and classification	98.5
Proposed ACO-CNN	99.5

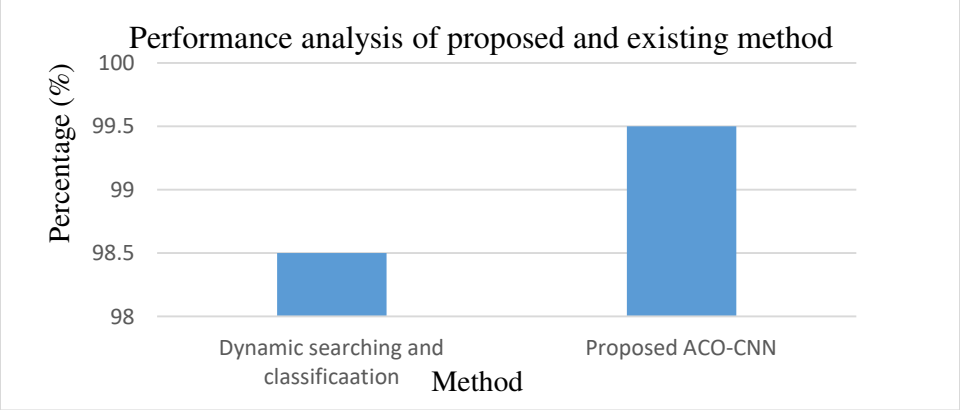

Figure 6: **Performance analysis of proposed and existing method**

| e-ISSN: 2320-9801, p-ISSN: 2320-9798| www.ijircce.com | |Impact Factor: 8.165

|| Volume 10, Issue 9, September 2022 ||

| DOI: 10.15680/IJIRCCE.2022.1009031 |

The proposed ACO-CNN method is compared with the dynamic searching and classification method and the results show that the accuracy of ACO-CNN is 99.5% which is higher than the dynamic searching and classification method which has an accuracy of 98.5%. It is represented in figure.6.

The proposed technique Ant Colony Optimization-based Convolutional Neural Network achieves superior efficiency when matched with previously implemented highlight removal techniques like dynamic searching and classification, automatic and single camera robust, dichromatic reflection model, light weight optimization, hardware implementation, and multiband polarization which is tabularized in table 4. The advanced AC0-based Convolutional Neural Network shows improved accuracy than the performance evaluated by employing Ant Colony Optimization as well as Convolutional Neural Networks individually. Here the achieved accuracy level is 98.95%using the ACO-CNN model. This represents that ACO relies onCNN that can be utilized to remove the highlights from the hyperspectral images.

VI. CONCLUSION

One of the emerging technologies in the field of hyperspectral imaging is image processing. Despite that in some conditions, the formation of highlights in hyperspectral images will make it indefinite. So,to categorize, characterize, and segment, the employed technique was therefore mainly focused on the removal of highlights from the hyperspectral images. Several datasets containing hyperspectral images are acquired and they are examined. To remove the unwanted noise and effects in hyper spectra images, a hybrid filter called the Weinmed filter is employed in the preprocessing stage.Then GLCM is used in the feature extraction stage to characterize the attributes of an image by calculating how often a pair of pixels with specific values occur in an image.Furthermore, the employed ACO-CNN technique is utilized to segment the highlighted region while detecting the highlights in hyperspectral images using a Convolutional Neural Network (CNN). Better detection and prediction accuracy is also reached using ACO-CNN. Then the highlighted region is removed using the constrained spectral unmixing method. Therefore, the prediction accuracy of the proposed method was found to be 99.5 percent.The efficiency can be enhanced by introducing a deep learning technique based on the combination of Long Short-Term Memory (LSTM) and Convolutional Neural Network (CNN).

REFERENCES

[1] S. M. Alsaleh, A. I. Aviles, P. Sobrevilla, A. Casals, and J. K. Hahn, “Automatic and robust single-camera specular highlight removal in cardiac images,” in *2015 37th Annual International Conference of the IEEE Engineering in Medicine and Biology Society (EMBC)*, Milan, Aug. 2015, pp. 675–678. doi: 10.1109/EMBC.2015.7318452.

[2] J. Hao, Y. Zhao, and Q. Peng, “A Specular Highlight Removal Algorithm for Quality Inspection of Fresh Fruits,” p. 24, 2022.

[3] V. S. Ramos, L. G. D. Q. Silveira Junior, and L. F. D. Q. Silveira, “Single Image Highlight Removal for Real-Time Image Processing Pipelines,” *IEEE Access*, vol. 8, pp. 3240–3254, 2020, doi: 10.1109/ACCESS.2019.2963037.

[4] Y. Gao *et al.*, “Dynamic Searching and Classification for Highlight Removal on Endoscopic Image,” *Procedia Comput. Sci.*, vol. 107, pp. 762–767, 2017, doi: 10.1016/j.procs.2017.03.161.

[5] D. Ngo, S. Lee, Q.-H. Nguyen, T. M. Ngo, G.-D. Lee, and B. Kang, “Single Image Haze Removal from Image Enhancement Perspective for Real-Time Vision-Based Systems,” *Sensors*, vol. 20, no. 18, p. 5170, Sep. 2020, doi: 10.3390/s20185170.

[6] Q. Yang, S. Wang, and N. Ahuja, “Real-Time Specular Highlight Removal Using Bilateral Filtering,” p. 14.

[7] T. Su, Y. Zhou, Y. Yu, and S. Du, “Highlight Removal of Multi-View Facial Images,” *Sensors*, vol. 22, no. 17, p. 6656, Sep. 2022, doi: 10.3390/s22176656.

[8] J. Gu *et al.*, “Recent advances in convolutional neural networks,” *Pattern Recognit.*, vol. 77, pp. 354–377, May 2018, doi: 10.1016/j.patcog.2017.10.013.

| e-ISSN: 2320-9801, p-ISSN: 2320-9798| www.ijircce.com | |Impact Factor: 8.165

|| Volume 10, Issue 9, September 2022 ||

| DOI: 10.15680/IJIRCCE.2022.1009031 |

[9] C. Rao and Y. Liu, "Three-dimensional convolutional neural network (3D-CNN) for heterogeneous material homogenization," *Comput. Mater. Sci.*, vol. 184, p. 109850, Nov. 2020, doi: 10.1016/j.commatsci.2020.109850.
[10] C. Blum, "Ant colony optimization: Introduction and recent trends," *Phys. Life Rev.*, vol. 2, no. 4, pp. 353–373, Dec. 2005, doi: 10.1016/j.plrev.2005.10.001.
[11] K. Khanna and S. Madan Arora, "Ant Colony Optimization towards Image Processing," *Indian J. Sci. Technol.*, vol. 9, no. 48, Dec. 2016, doi: 10.17485/ijst/2016/v9i48/105784.
[12] J. Suo, D. An, X. Ji, H. Wang, and Q. Dai, "Fast and High Quality Highlight Removal From a Single Image," *IEEE Trans. Image Process.*, vol. 25, no. 11, pp. 5441–5454, Nov. 2016, doi: 10.1109/TIP.2016.2605002.
[13] A. C. S. Souza, M. C. F. Macedo, V. P. Nascimento, and B. S. Oliveira, "Real-Time High-Quality Specular Highlight Removal Using Efficient Pixel Clustering," in *2018 31st SIBGRAPI Conference on Graphics, Patterns and Images (SIBGRAPI)*, Parana, Oct. 2018, pp. 56–63. doi: 10.1109/SIBGRAPI.2018.00014.
[14] A. Nikonorov, S. Bibikov, V. Myasnikov, Y. Yuzifovich, and V. Fursov, "Correcting color and hyperspectral images with identification of distortion model," *Pattern Recognit. Lett.*, vol. 83, pp. 178–187, Nov. 2016, doi: 10.1016/j.patrec.2016.06.027.
[15] W. Xia, E. C. S. Chen, S. E. Pautler, and T. M. Peters, "A Global Optimization Method for Specular Highlight Removal From a Single Image," *IEEE Access*, vol. 7, pp. 125976–125990, 2019, doi: 10.1109/ACCESS.2019.2939229.
[16] P. Topno and G. Murmu, "An Improved Edge Detection Method based on Median Filter," in *2019 Devices for Integrated Circuit (DevIC)*, Kalyani, India, Mar. 2019, pp. 378–381. doi: 10.1109/DEVIC.2019.8783450.
[17] C. Ma, X. Lv, and J. Ao, "Difference based median filter for removal of random value impulse noise in images," *Multimed. Tools Appl.*, vol. 78, no. 1, pp. 1131–1148, Jan. 2019, doi: 10.1007/s11042-018-6442-2.
[18] J. Lv, F. Wang, L. Xu, Z. Ma, and B. Yang, "A segmentation method of bagged green apple image," *Sci. Hortic.*, vol. 246, pp. 411–417, Feb. 2019, doi: 10.1016/j.scienta.2018.11.030.
[19] O. Eches, J. A. Benediktsson, N. Dobigeon, and J. Tourneret, "Adaptive Markov Random Fields for Joint Unmixing and Segmentation of Hyperspectral Images," *IEEE Trans. Image Process.*, vol. 22, no. 1, pp. 5–16, Jan. 2013, doi: 10.1109/TIP.2012.2204270.
[20] J. Nalepa, M. Myller, Y. Imai, K.-I. Honda, T. Takeda, and M. Antoniak, "Unsupervised Segmentation of Hyperspectral Images Using 3-D Convolutional Autoencoders," *IEEE Geosci. Remote Sens. Lett.*, vol. 17, no. 11, pp. 1948–1952, Nov. 2020, doi: 10.1109/LGRS.2019.2960945.
[21] D. Levine, "Feature Extraction: A Survey," p. 17.
[22] P. Koirala, P. Pant, M. Hauta-Kasari, and J. Parkkinen, "Highlight detection and removal from spectral image," *J. Opt. Soc. Am. A*, vol. 28, no. 11, p. 2284, Nov. 2011, doi: 10.1364/JOSAA.28.002284.
[23] Chein-I Chang, "Orthogonal subspace projection (OSP) revisited: a comprehensive study and analysis," *IEEE Trans. Geosci. Remote Sens.*, vol. 43, no. 3, pp. 502–518, Mar. 2005, doi: 10.1109/TGRS.2004.839543.
[24] D. Kim and I.-B. Lee, "Process monitoring based on probabilistic PCA," *Chemom. Intell. Lab. Syst.*, vol. 67, no. 2, pp. 109–123, Aug. 2003, doi: 10.1016/S0169-7439(03)00063-7.
[25] C. Shi and L. Wang, "Incorporating spatial information in spectral unmixing: A review," *Remote Sens. Environ.*, vol. 149, pp. 70–87, Jun. 2014, doi: 10.1016/j.rse.2014.03.034.

INNO SPACE
SJIF Scientific Journal Impact Factor

Impact Factor: 8.165

doi cross ref

ISSN INTERNATIONAL STANDARD SERIAL NUMBER INDIA

निस्केयर NISCAIR

INTERNATIONAL JOURNAL OF INNOVATIVE RESEARCH

IN COMPUTER & COMMUNICATION ENGINEERING

9940 572 462 6381 907 438 ijircce@gmail.com

www.ijircce.com

Scan to save the contact details